Chaos
An Interdisciplinary Journal of Nonlinear Science

RESEARCH ARTICLE | OCTOBER 12 2023

Integrability and dynamics of a simplified class B laser system

J. Llibre ; C. Pantazi

Chaos 33, 103119 (2023)
https://doi.org/10.1063/5.0169342

AIP Publishing

Integrability and dynamics of a simplified class B laser system

Cite as: Chaos 33, 103119 (2023); doi: 10.1063/5.0169342
Submitted: 25 July 2023 · Accepted: 21 September 2023 ·
Published Online: 12 October 2023

J. Llibre[1,a] and C. Pantazi[2,b]

AFFILIATIONS

[1]Dept. Matemàtiques, Universitat Autònoma de Barcelona, 08193 Bellaterra, Barcelona, Catalonia, Spain
[2]Departament de Matemàtiques, Universitat Politècnica de Catalunya, (EPSEB), Av. Doctor Marañón, 44–50, 08028 Barcelona, Spain

[a)]jllibre@mat.uab.cat
[b)]**Author to whom correspondence should be addressed:** chara.pantazi@upc.edu

ABSTRACT

A simplified class B laser system is a family of differential polynomial systems of degree two depending on the parameters a and b. Its rich dynamics has already been observed in 1980s, see Arecchi *et al.* [Opt. Commun. **51**, 308–314 (1984)] and Politi *et al.* [Phys. Rev. A **33**, 4055 (1986)], and still nowadays, it attracts the interest of the researchers. In this paper, we characterize its dynamics near infinity for all values of the parameters. When $a = 0$, the partial integrability was already proved by Oppo and Politi [Z. Phys. B Con. Mat. **59**, 111–115 (1985)]. Here, we prove that for $a = 0$, it is completely integrable with two independent first integrals given by Liouvillian functions, and we present a complete study of its dynamics. When $a \neq 0$, we study its dynamics in the Poincaré ball $\mathbb{B}^3$, i.e., the interior of this ball is identified with $\mathbb{R}^3$ and its boundary the two-dimensional sphere $\mathbb{S}^2$ is identified with the infinity of $\mathbb{R}^3$.

A laser is a device that emits light after stimulation of atoms or molecules. It is a key component of many everyday products with further uses in manufacturing and in medical procedures. In particular, a simplified class B laser system is a two parametric family of nonlinear differential equations in three dimensions that since 1980s attracts the interest of the researchers. In this work, we characterize completely its dynamics near the infinity for all values of the parameters using the Poincaré ball $\mathbb{B}^3$. Our results, purely analytic, are in accordance with some numerical results already appeared in the literature. When a parameter is zero, we succeed to prove the complete integrability of this system, and hence, we improve some previous known results. We note that for $a = 0$, the partial integrability is already proved in Ref. 1.

I. INTRODUCTION AND STATEMENT OF THE MAIN RESULT

The word LASER is an acronym for Light Amplification by Stimulated Emission of Radiation. It is a device that stimulates atoms or molecules to emit light at particular wavelengths and amplifies that light, producing a very narrow beam of radiation. Lasers are used in optical disk drives, laser printers, barcode scanners, DNA sequencing instruments, fiber-optic, and free-space optical communication, semiconducting chip manufacturing, laser surgery and skin treatments, cutting and welding materials, and in laser lighting displays.

Lasers are typical models that can be described using nonlinear dynamics. In 1984, the authors of Ref. 2 classify the lasers into following three classes according to the damping rates $\gamma_\perp, \gamma_{\shortparallel}$, and k (rates of polarization, population, and field, respectively); see for more details, Ref. 3.

Class A: $\gamma_\perp \simeq \gamma_{\shortparallel} \gg k$. Polarization and population decay much faster than the field, and the dynamics are governed by a single field equation.

Class B: $\gamma_\perp \gg k \gtrsim \gamma_{\shortparallel}$. The population decays slowly, so that the dynamics are described by two coupled rate equations. By injection of an external signal into a homogeneous line, the dynamics can be described by a system of three nonlinear coupled equations.

Class C: $\gamma_{\shortparallel} \simeq \gamma_\perp \simeq k$. The three decay rates for polarization, population, and field are of the same order of magnitude.

In particular, class B lasers become reliable devices for studying chaos and generalized multistability; see Ref. 4.

Although in the last years multi-mode systems attracted the interest of many researchers, here we will restrict our study of a single mode laser. The dynamics of a laser with an external signal are of an important consideration in the literature. In Ref. 5, a modified set of equations for class B laser with an injected signal is studied. A second-order perturbation is applied and indicates the existence of an anomalous pushing of the laser frequency. This phenomenon is confirmed by the numerical analysis. In Ref. 6, the authors concern the locked–unlocked transition for their model, and very rich dynamics appear due to the combination of local and global effects. A Silnikov–saddle–node interaction appears in Ref. 7 and is related to the chaotic behavior. A systematic order-by-order analysis is presented in Ref. 8, and there is a complex structure of homoclinic and heteroclinic connections due to the existence of an unstable periodic orbit.

Moreover, in Ref. 9, the authors introduced the following model to describe the class-B laser with externally injected signal,

$$\begin{aligned} \dot{\phi} &= -\Theta - \frac{E_0 \sin\phi}{E}, \\ \dot{E} &= wE + E_0 \cos\phi, \\ \dot{w} &= d - E^2 - \varepsilon\left(1 + E^2\right) w, \end{aligned} \tag{1}$$

with time $\tau = \sqrt{k\gamma_{\parallel}}\, t$. The variable E denotes the cavity field amplitude, ϕ is its phase, and w is the population inversion. The parameter Θ denotes the cavity mistuning, E_0 is the Rabi frequence of the external field, d is the pump parameter referred to the threshold value, and $\varepsilon = \sqrt{\gamma_{\parallel} k}$. System (1) is a special case of a model in Ref. 2 where the authors found numerical evidence of chaos, and this fact motivates many new studies.

Additionally, in Ref. 9, it is showed that the model (1) can be approximately described (considering the limit case $\varepsilon = 0$) by the following reversible three-dimensional system:

$$\begin{aligned} \dot{x} &= xz + y + a, \\ \dot{y} &= yz - x, \\ \dot{z} &= b - x^2 - y^2, \end{aligned} \tag{2}$$

where there is a rescaling of time by Θ, it is written in cartesian coordinates, and the new parameters are $a = E_0/\Theta^2$ and $b = d/\Theta^2$. An important result of Ref. 9 is that for suitable parameter ranges, conservative and dissipative behavior are observed.

Some very recent papers (Refs. 10 and 11) provide information about the dynamics and the integrability of system (2). Our goal here is to complete the study of the integrability of system (2) and provide more information about its dynamics.

System (2) is invariant under the symmetry $(x, y, z, t) \to (-x, y, -z, -t)$, as already was noted in Ref. 9. Hence, the orbits of the system are symmetric with respect to the y-axis.

We associate to system (2) its vector field

$$\mathcal{X} = (xz + y + a)\frac{\partial}{\partial x} + (yz - x)\frac{\partial}{\partial y} + \left(b - x^2 - y^2\right)\frac{\partial}{\partial z}.$$

Let Ω be an open subset of $\mathbb{R}^3$ and let $\mathcal{X} : \Omega \to \mathbb{R}^3$ be the vector field associated to system (2). Consider $p \in \Omega$ and we denote by $\Phi(t) = \Phi(t, p) = \Phi_p(t)$ the integral curve of X passing through the point p when $t = 0$. We define the sets

$$\begin{aligned} \omega(p) = \big\{ & q \in \Omega : \text{there exist } \{t_n\} \quad \text{with} \quad t_n \to \infty \quad \text{and} \\ & \Phi(t_n) \to q \quad \text{when} \quad n \to \infty \big\}, \\ \alpha(p) = \big\{ & q \in \Omega : \text{there exist } \{t_n\} \quad \text{with} \quad t_n \to -\infty \quad \text{and} \\ & \Phi(t_n) \to q \quad \text{when} \quad n \to \infty \big\}. \end{aligned}$$

The sets $\omega(p)$ and $\alpha(p)$ are called the *ω–limit set* and the *α-limit set of p*, respectively.

Let U be an open set of $\mathbb{R}^3$. We say that a non-locally constant analytic function $H : U \to \mathbb{R}$ is a *first integral* of system (2) in U if it is constant on all the orbits of the system contained in U. Thus, the function H is a first integral of system (2) in U if and only if

$$\begin{aligned} \dot{H} = \frac{dH}{dt} = \mathcal{X}H = (xz + y + a)\frac{\partial H}{\partial x} + (yz - x)\frac{\partial H}{\partial y} \\ + \left(b - x^2 - y^2\right)\frac{\partial H}{\partial z} = 0, \end{aligned}$$

in all the points of U. Roughly speaking, a *Liouvillian first integral* is a first integral obtained by a combination of algebraic functions, integrals, and exponential of integrals of elementary functions; for a precise definition, see Ref. 12.

Two local first integrals H_1 and H_2 defined in U are *independent* if their gradients are linearly independent in $\mathbb{R}^3$ except perhaps in a set of measure zero.

The knowledge of a first integral is very useful for understanding the dynamics of system (2). Next theorem provides the expressions of two functionally independent first integrals when the parameter a is zero and improves the results of Refs. 1 and 10 where the partial integrability is proved giving the expression of only one first integral.

Theorem 1. *The differential system (2) for $a = 0$ is completely integrable with the following two functionally independent first integrals:*

(a) *If $a = 0$ and $b \neq 0$,*

$$H_1(x, y, z) = \frac{\left(x^2 + y^2\right)^b}{e^{x^2+y^2+z^2}},$$

$$H_2(x, y, z) = 2\arctan\left(\frac{x}{y}\right) - \int_0^{x^2+y^2} \frac{1}{s\sqrt{b\ln(s) - \ln\left(e^{-x^2-y^2-z^2}\left(x^2 + y^2\right)^b\right) - s}}\, ds.$$

(b) *For* $a = b = 0$,

$$H_1(x,y,z) = x^2 + y^2 + z^2,$$
$$H_2(x,y,z) = \frac{\exp\left(2\sqrt{x^2+y^2+z^2}\,\arctan\left(\frac{y}{x}\right)\right)\left(\sqrt{x^2+y^2+z^2}-z\right)^2}{x^2+y^2}.$$

The next result characterizes the dynamics of system (2) on sphere $\mathbb{S}^2$ of the infinity. For more details on Poincaré compactification, the infinity sphere $\mathbb{S}^2$, and the notations for studying on it the dynamics of the system, see the Appendix.

Proposition 2. *The following statements hold.*

(i) *The origin* $P = (0,0,0)$ *of the local chart* (U_3, F_3) *and the origin* $P' = (0,0,0)$ *of the local chart* (V_3, G_3) *are the unique infinite equilibrium points.*
(ii) *All the orbits on the infinity* $\mathbb{S}^2$ *of the Poincaré ball* $\mathbb{B}^3$ *have* α*-limit the point* P *and* ω*-limit the point* P'.

In the next result, we classify the finite equilibrium points of system (2).

Proposition 3. *The next statements hold.*

(i) *If* $a = 0$ *and* $b \neq 0$, *system (2) has no finite equilibrium points.*
(ii) *If* $a = 0$ *and* $b = 0$, *the z-axis if filled with equilibrium points.*
(iii) *If* $a \neq 0$ *and* $b \leq 0$, *system (2) has no finite equilibrium points.*
(iv) *If* $0 < b < a^2$, *system (2) has the following two equilibrium points:*

$$P_1 = \left(\frac{\sqrt{b(a^2-b)}}{a}, -\frac{b}{a}, -\frac{\sqrt{b(a^2-b)}}{b}\right),$$
$$P_2 = \left(-\frac{\sqrt{b(a^2-b)}}{a}, -\frac{b}{a}, \frac{\sqrt{b(a^2-b)}}{b}\right). \quad (3)$$

P_1 is an attractor and P_2 is a repeller. Moreover, P_1 (resp. P_2) bifurcates from the infinite equilibrium point P' (resp. P) at $b = 0$.
(v) *If* $b = a^2 > 0$, *the two equilibrium points P_1 and P_2 collide at the finite equilibrium point* $Q = (0, -a, 0)$ *with eigenvalues* $0, \pm\sqrt{-2a^2-1}$.
(vi) *If* $b > a^2 > 0$, *there are no finite equilibrium points.*

The case $a = b = 0$ corresponds to the laser with no injection at the laser threshold. From Proposition 3(ii), we have that the z-axis is filed with equilibrium points, and this corresponds to the zero emission state with undefined phase.

The next theorem characterizes the phase portraits of system (2) when $a = b = 0$.

Theorem 4. *The phase portrait in* $\mathbb{R}^3$ *of the differential system (2) when* $a = b = 0$ *is as follows:*

(a) *The origin of coordinates is an equilibrium point.*
(b) *All the spheres* $x^2 + y^2 + z^2 = r^2 > 0$ *centered at the origin of coordinates are invariant by the flow of the differential system.*
(c) *There is an unstable focus at the north pole of the sphere* $x^2 + y^2 + z^2 = r^2 > 0$ *and a stable focus at the south pole.*
(d) *Every orbit of the invariant sphere* $x^2 + y^2 + z^2 = r^2 > 0$ *different from the two poles is a spiral starting at the north pole and ending at the south pole.*

Statement (d) of Theorem 4 shows a mistake in Theorem 4 of Ref. 10, where the author states that any integral surface $x^2 + y^2 + z^2 = \varepsilon^2$ contains at least one periodic solution when $\varepsilon > 0$ and small.

Consider now $a = 0$ and $b \neq 0$. In cylindrical coordinates, system (2) becomes

$$\dot{r} = rz, \quad \dot{\theta} = -1, \quad \dot{z} = b - r^2. \quad (4)$$

According to Theorem 1(b), system (4) admits the first integral $H_1(r,\theta,z) = r^{2b}/e^{r^2+z^2}$. Consider the level set $H_1 = h$ with $h \geq 0$. In the next theorem, we study the phase portraits of system (4) over the invariant surfaces $r^{2b} = he^{r^2+z^2}$.

Theorem 5. *The phase portrait in* $\mathbb{R}^3$ *of the differential system (4) when* $b \neq 0$ *is as follows:*

(a) *If* $b > 0$ *and* $h = 0$, *the level* $H_1 = 0$ *reduces to the invariant z-axis, where there is an orbit coming from* $z = -\infty$ *and going to* $z = +\infty$.
(b) *If* $b > 0$ *and* $h \in (0, b^b e^{-b})$, *then the invariant surface* $H_1 = h$ *is a topological torus surrounding the z-axis. On this invariant torus, either the orbits close and are periodic, or the orbits are dense in the torus.*
(c) *If* $b > 0$ *and* $h = b^b e^{-b}$, *then the level* $H_1 = b^b e^{-b}$ *is a periodic orbit of radius* $\sqrt{b}$ *in the plane* $z = 0$.
(d) *If* $b < 0$ *and* $h = 0$, *then the level* $H_1 = 0$ *reduces to the invariant z-axis, where there is an orbit coming from* $z = +\infty$ *and goes to* $z = -\infty$.
(e) *If* $b < 0$ *and* $h > 0$, *then the invariant surface* $H_1 = h$ *is a topological cylinder surrounding the z-axis. On this cylinder, the orbits come from the* $z = +\infty$ *and go to* $z = -\infty$ *rotating in clockwise sense.*

Remark 6. *Taking* $s = \ln r$ *in system (4), we obtain the second-order differential equation,*

$$\ddot{s} + e^{2s} - b = 0,$$

that is, the Toda oscillator of Ref. 13. Now considering the new variables $q = 2s - \ln b$ *and* $\tau = (2b)^{1/2}t$. *We have*

$$\frac{d^2q}{d\tau^2} = 1 - e^q, \quad (5)$$

and Eq. (5) already appears in Ref. 1 and admits the invariant of motion,

$$E \equiv \frac{1}{2}\left(\frac{dq}{d\tau}\right)^2 - q + e^q - 1 = \frac{z^2}{b} + \frac{r^2}{b} - \ln\left(\frac{r^2}{b}\right) - 1.$$

Note that E is also a first integral of system (4). We recall that system (4) admits the first integral $H_1 = r/e^{r^2+z^2}$, *and we have* $e^E = b \Big/ \left(eH_1^{\frac{1}{b}}\right)$.

In the next theorem for $a \neq 0$, we characterize the phase portraits of system (2) in $\mathbb{B}^3$.

Theorem 7. *The phase portraits in* $\mathbb{B}^3$ *of the differential system (2) for* $a \neq 0$ *are as follows:*

(a) *If* $b \leq 0$. *All the orbits are heteroclinic starting at the equilibrium point P and ending at the equilibrium point P′.*
(b) *If* $0 < b < a^2$. *There are heteroclinic orbits starting at the equilibrium point P and ending at the equilibrium point P′. Additionally, we have found numerically that there are heteroclinic orbits between the equilibria P and P′.*
(c) *If* $b = a^2 > 0$. *There are heteroclinic orbits starting at the equilibrium point* P_1 *and ending at the equilibrium point* P_2. *Additionally, there are homoclinic orbits to the equilibria Q and some periodic orbits.*
(d) *If* $b > a^2 > 0$. *There are heteroclinic orbits starting at the north pole of the ball* $\mathbb{B}^3$ *and ending on its south pole, and there are some periodic orbits.*

II. PROOF OF THE RESULTS

A. The Poincaré compactification and the infinite equilibrium points

The Poincaré ball $\mathbb{B}^3$, roughly speaking, is the closed ball of radius one centered at the origin of coordinates of $\mathbb{R}^3$. Its interior is identified with $\mathbb{R}^3$ and its boundary, the two-dimensional sphere $\mathbb{S}^2$, is identified with the infinity of $\mathbb{R}^3$, because in $\mathbb{R}^3$ we can go to infinity in as many directions as points have $\mathbb{R}^3$. For more details, see the Appendix.

Proof of Proposition 2. From the Appendix in the local chart (U_1, F_1), the compactified polynomial differential system (2) is

$$\begin{aligned}\dot{z}_1 &= -z_3\left(az_1z_3 + z_1^2 + 1\right),\\ \dot{z}_2 &= -az_2\,z_3^2 + b\,z_3^2 - z_1z_2z_3 - z_1^2 - z_2^2 - 1,\\ \dot{z}_3 &= -z_3\left(a\,z_3^2 + z_1z_3 + z_2\right),\end{aligned}$$

and in $z_3 = 0$, there are no equilibrium points, so in the local chart (U_1, F_1) there are no infinite equilibria.

In the local chart (U_2, F_2), system (2) becomes

$$\begin{aligned}\dot{z}_1 &= z_3\left(az_3 + {z_1}^2 + 1\right),\\ \dot{z}_2 &= b\,z_3^2 + z_1z_2z_3 - z_1^2 - z_2^2 - 1,\\ \dot{z}_3 &= z_3\left(z_1z_3 - z_2\right),\end{aligned}$$

and again, there are no infinite equilibrium points in the chart (U_2, F_2).

The origin $(0, 0, 0)$ of the local chart (U_3, F_3) is the unique infinite equilibrium point in the chart as we get from the equations of the compactified system (2) in this chart,

$$\begin{aligned}\dot{z}_1 &= -bz_1\,z_3^2 + a\,z_3^2 + z_1^3 + z_1\,z_2^2 + z_2z_3 + z_1,\\ \dot{z}_2 &= -bz_2\,z_3^2 + z_1^2z_2 + z_2^3 - z_1z_3 + z_2,\\ \dot{z}_3 &= -z_3\left(b\,z_3^2 - z_1^2 - z_2^2\right).\end{aligned}$$

The linear part at $(0, 0, 0)$ of this system is

$$\begin{bmatrix}1 & 0 & 0\\ 0 & 1 & 0\\ 0 & 0 & 0\end{bmatrix},$$

and the eigenvalues of the matrix are $1, 1, 0$. So the north pole of the sphere $\mathbb{S}^2$ is an unstable node. Hence, the origin of the local chart V_3, i.e., the south pole of $\mathbb{S}^2$, is an unstable node. This completes the proof of Proposition 2. □

B. Finite equilibrium points

Here, we present the proof of Proposition 3 that characterize the finite equilibrium points of system (2).

Proof. First, we consider $a = 0$.

(i) $b \neq 0$. System (2) has no finite equilibrium points.
(ii) $b = 0$. The z-axis $\{(0, 0, z), z \in \mathbb{R}\}$ is filled with equilibrium points.

Now we consider $a \neq 0$. We distinguish the following cases:

(iii) $b \leq 0$. System (2) has no finite equilibrium points.
(iv) For $b \gtrsim 0$. Two finite equilibrium points, P_1 and P_2, bifurcate from the infinity. The point P_1 born from the south pole and the point P_2 born from the north pole. For $0 < b < a^2$. The expressions of the two finite equilibrium points are given in (3). The characteristic polynomial of the Jacobian matrix at the equilibrium point P_1 is

$$\lambda^3 + \frac{2\sqrt{b\left(a^2 - b\right)}\,\lambda^2}{b} + \frac{\left(a^2 + 2b^2\right)\lambda}{b} + 2\sqrt{b\left(a^2 - b\right)},$$

and from the Routh–Hurwitz criterium, we have that all the eigenvalues have negative real parts, and so the point P_1 is an attractor. Since system (2) admits the symmetry $(x, y, z, t) \to (-x, y, -z, -t)$, we have that the equilibrium point P_2 is a repeller.
(v) $b = a^2 > 0$. The two finite equilibrium points collapse and now we have one equilibrium point $Q = (0, -a, 0)$. The Jacobian matrix at the point Q is

$$\begin{bmatrix}0 & 1 & 0\\ -1 & 0 & -a\\ 0 & 2a & 0\end{bmatrix},$$

and its eigenvalues are $0, \pm\sqrt{-2a^2 - 1}$.
(vi) $b > a^2 > 0$. System (2) has no finite equilibrium points.

This completes the proof of Proposition 3. □

C. Phase portraits of system (2) in $\mathbb{R}^3$ when $a = 0$.

Proof of Theorem 4. Consider $a = b = 0$ in system (2). Then, from Theorem 1(b), system (2) has the first integral $H_1(x, y, z) = x^2 + y^2 + z^2$. Hence the space $\mathbb{R}^3$ is foliated by the invariant spheres $x^2 + y^2 + z^2 = r^2 > 0$. The z-axis is filled with equilibrium points. So, in particular, the origin of coordinates is an equilibrium point. Therefore, statements (a) and (b) are proved.

Now over each invariant sphere, the equilibrium point $(0, 0, r)$ has eigenvalues $0, r + i, r - i$, so it is an unstable focus, and the equilibrium point $(0, 0, -r)$ has eigenvalues $0, -r + i, -r - i$, and is a stable focus. Since $\dot{z} = -(x^2 + y^2) < 0$ on all the points of the invariant sphere, except at its two poles, every orbit is a spiral that starts at the north pole and end at the south pole. So statements (c) and (d) are proved. □

Proof of Theorem 5. First consider $b > 0$. For $h = 0$, the energy level $H_1 = 0$ yields to $r = 0$ and so it reduces to the invariant z-axis. Since $\dot{z} = b > 0$, there is an orbit coming from $z = -\infty$ and goes to $z = +\infty$, and so statement (a) is proved.

For $h \gtrsim 0$ and $h \in (0, b^b e^{-b})$, the energy level $H_1 = h$ yields to $z^2 = \log(r^{2b}/h) - r^2$ and in the (r, z) plane is an oval, see Fig. 1(a). Moreover, for $z > 0$, we have $\dot{r} > 0$, and for $z < 0$, we have $\dot{r} < 0$. So on the oval, the orbits rotate in a clockwise sense. In $\mathbb{R}^3$, since $\dot{\theta} = -1$, from the oval we obtain that the energy level is a topological torus surrounding the z-axis. On this torus we define meridians and parallels as in Fig. 1(b). Note that on the torus, the orbits have two movements of rotation; one running the meridians in the clockwise sense and the other one running parallel also in the clockwise sense. So the orbits of system (4) follow these two rotations, and either close and are periodic, or are dense, see Fig. 1(b). This is because the Poincaré map over the invariant torus defined on the circle $\theta = 0$ is a diffeomorphism. Such diffeomorphism has a rotation number. If it is rational, all the orbits on the torus are periodic, and if it is irrational, all the orbits on the torus are dense. For more details, see Ref. 14. Now while h increases, the torus becomes smaller. This completes the proof of statement (b).

For $h = b^b e^{-b}$ and $z = 0$, we have $\dot{r} = 0$, and from the level set $H_1 = b^b e^{-b}$, we obtain $r = \sqrt{b}$, so the torus collapses to a circle and system (4) becomes $\dot{r} = 0, \dot{\theta} = -1, \dot{z} = 0$, and the energy level is formed by a periodic orbit. This completes the proof of statement (c).

We note that the tori correspond to the levels $H_1 = h$ with $h \in (0, b^b e^{-b})$. When $h \gtrsim 0$ the tori tends to infinity and when $h \nearrow b^b e^{-b}$, the tori collapse to the periodic orbit of the statement (c). Such periodic orbit is in the interior of the region limited by all the tori.

Now consider $b < 0$.

For $h = 0$, the energy level $H_1 = 0$ yields to $r = 0$, and so it reduces to the invariant z-axis. Since $\dot{z} = b < 0$, there is an orbit coming from $z = +\infty$ and goes to $z = -\infty$, and so statement (d) is proved.

For $h > 0$, the level set $H_1 = h$ in the (r, z) plane is the curve shown in Fig. 2(a) and in $\mathbb{R}^3$ gives rise to a cylinder. On this cylinder since $\dot{z} < 0$, the orbits come from the $z = +\infty$ and go to $z = -\infty$, and since $\dot{\theta} = -1$, they are rotating in the clockwise sense. This completes the proof of statement (e). □

D. Phase portraits on the Poincaré ball $\mathbb{B}^3$ for $a \neq 0$.

Proof of Theorem 7. We distinguish the following cases for $a \neq 0$.

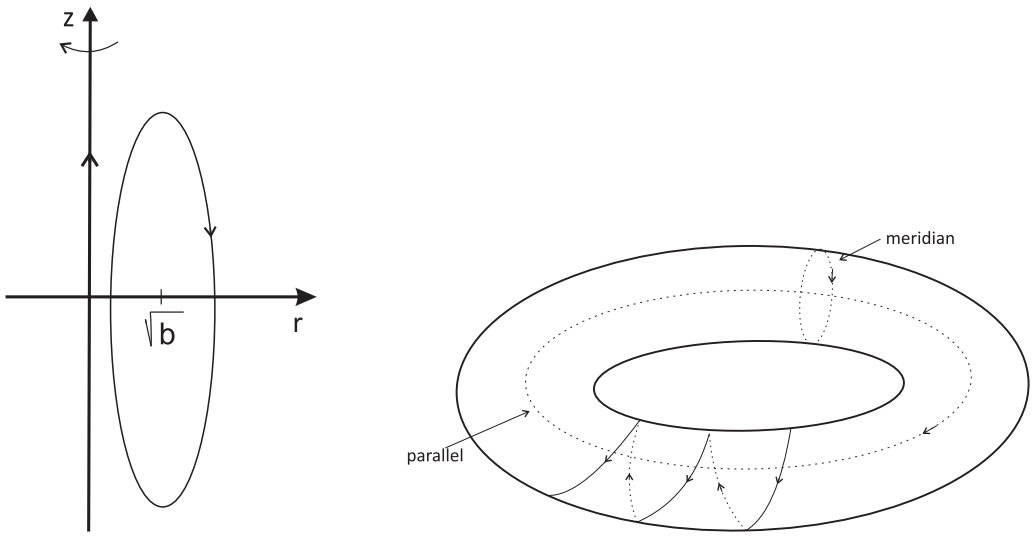

(a) (b)

FIG. 1. $b > 0$.

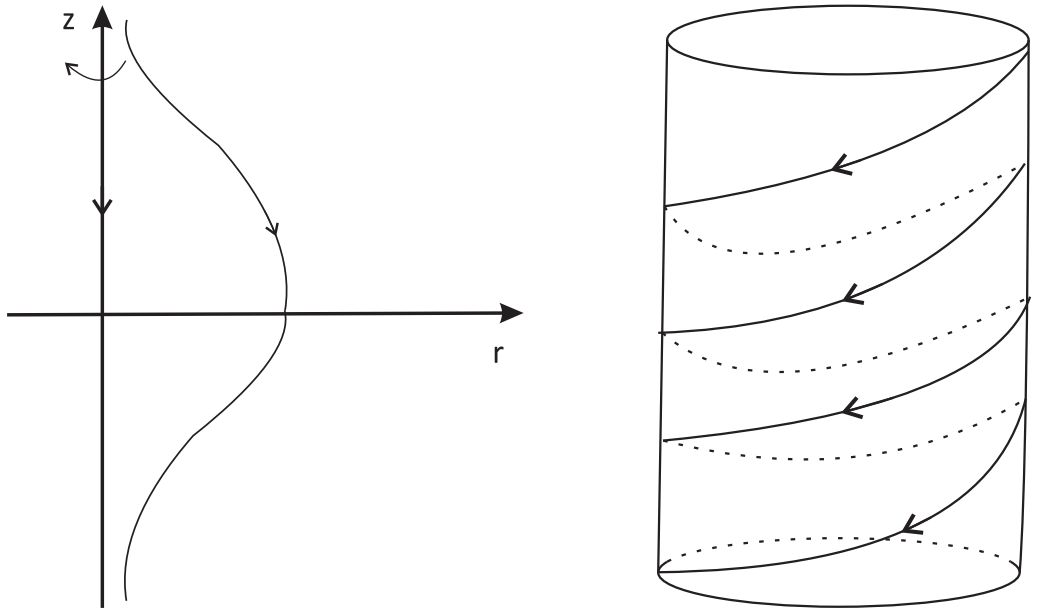

FIG. 2. $b < 0$.

Case $b < 0$. Note that for system (2), we have $\dot{z} < 0$ in $\mathbb{R}^3$, and if $b = 0$, then $\dot{z} < 0$ in $\mathbb{R}^3 \setminus \{(0, 0, z) : z \in \mathbb{R}\}$. So the α-limit of the orbits is the origin of the chart (U_3, F_3), namely the point P, whereas the ω–limit of the orbits is the origin of the chart (V_3, G_3), namely, the point P'. All the orbits are heteroclinic, see Fig. 3(a).

Case $0 < b < a^2$. Consider the cylinder $x^2 + y^2 = b$ or the cylinder $\dot{z} = 0$. Note that the two finite equilibrium points P_1 and P_2 are on this cylinder. From Proposition 2(ii) and since outside the cylinder $x^2 + y^2 = b$, we have $\dot{z} < 0$, as in the previous case, there are heteroclitic orbits near the sphere of the infinity $\mathbb{S}^2$ and far from the cylinder $x^2 + y^2 = b$, having α-limit the origin of the chart (U_3, F_3), namely, the north pole P, and having ω–limit the origin of the chart (V_3, G_3), namely the south pole point P', see Fig. 3(b). Numerically, we have found heteroclinic orbits with α-limit in the unstable point P_2 and ω-limit in the stable P_1. The dynamics between these two behaviors is complicated.

Case $b = a^2 > 0$. The finite equilibrium point $Q = (0, -a, 0)$ has eigenvalues $0, \pm\sqrt{-2a^2 - 1}$ and so is a zero-Hopf equilibrium point. In this case again there are heteroclinic orbits near the sphere of the infinity $\mathbb{S}^2$ and far from the cylinder $x^2 + y^2 = b$ with α-limit the equilibrium P and ω-limit the equilibrium P'. Some of the heteroclinic orbits going from P_2 to P_1 when $b \lesssim a^2$ now become homoclinic orbits at the point Q, see Fig. 3(c). Furthermore, numerically, we have detect some periodic orbit.

Case $b > a^2 > 0$. Consider the cylinder $x^2 + y^2 = b$ with $\dot{z} = 0$. There are also heteroclitic orbits near the sphere of the infinity $\mathbb{S}^2$ and far from the cylinder $x^2 + y^2 = b$, having α-limit the P and having ω-limit the P', see Fig. 3(d). Numerically, we know that for $b \gtrsim a^2$, there are periodic orbits. □

III. FINAL REMARKS

The class B laser system (2) introduced by Refs. 1, 2, 3, and 9 is already studied partially in more recent works like Refs. 10 and 11. Due to its rich dynamics, it attracts the interest of the researchers. Since 1980s as in Ref. 9, numerical evidence shows the coexistence of conservative and dissipative behavior of this system: The authors considered the realistic fixed values of $b = 4/3 = 1.333$ and $0 < a < 2/\sqrt{3} = 1.154\,700\,538$ in order to have physical meaning. Note that equilibrium points appear for $a = 2/\sqrt{3} = 1.154\,700\,538$. The authors detect numerically in system (2) the existence of invariant tori, period 2-solutions, and a period 11-solution. Additionally, the numerical results of the polynomial differential system (2) are in agreement with the behavior of the initial no polynomial differential system (1), see Ref. 9.

According to Proposition 3(iv), system (2) has the two finite equilibrium points P_1 (atractor) and P_2(repeller). According to Theorem 7(b), there are heteroclinic orbits starting at the infinite equilibrium point P and ending at the infinite equilibrium point P', and there are heteroclinic orbits between the equilibria P and P'.

In Ref. 11, the authors detect numerically the coexistence of dissipative and conservative flows of system (2). Concretely, they study the dynamics of system (2) for the fixed value $b = 1$. For $0 < a \leq 0.31$, the authors detect numerically that the motion is only

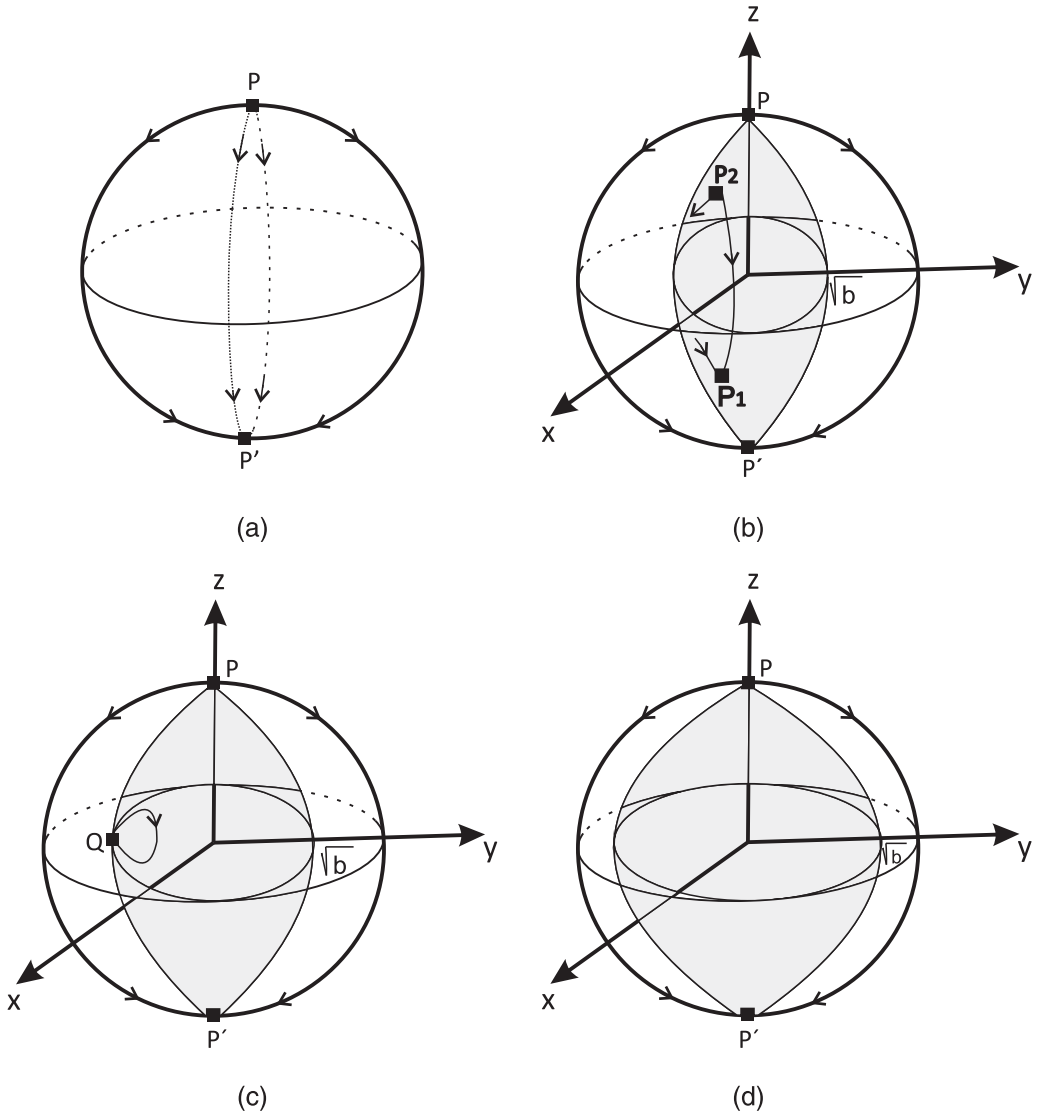

FIG. 3. The phase portraits of system (2) in the Poincaré ball $\mathbb{B}^3$ for $a \neq 0$.

volume conservative, while for $0.31 < a < 1$, it is additionally volume contractive. In Ref. 11, also they proved that for $a = b = 0$, system (2) is the energy conserved system. This is in accordance with our Theorems 1(b) and 4.

IV. CONCLUSIONS

In this paper, for first time in the literature, are proved the following results:

(i) System (2) for $a = 0$ is completely integrable and admits two functionally independent first integrals that are Liouvillian functions, see Theorem 1. This improves the known result about partially integrability proved already by Oppo and Politi in Ref. 1.

(ii) The dynamics of system (2) is described in the neighborhood of infinity, i.e., in the neighborhood of the infinite sphere $\mathbb{S}^2$. In particular, for all the values of the parameters a and $b \neq 0$, there are orbits that start at the infinite point at the end of the positive z-axis and end at the infinite point at the end of the negative z-axis, see Proposition 2 and Theorem 7.

(iii) The dynamics of system (2) have been completely described when the parameter $a = 0$, see Theorems 4 and 5.

ACKNOWLEDGMENTS

The first author was partially supported by the Agencia Estatal de Investigación Grant No. PID2019-104658GB-I00, the H2020 European Research Council Grant No. MSCA-RISE-2017-777911, AGAUR (Generalitat de Catalunya) Grant No. 2021SGR00113, and by the Acadèmia de Ciències i Arts de Barcelona. The second author was partially supported by the Ministerio de Ciencia e Innovación grant (No. PID2019-104658GB-I00) and by the Grant No. PID-2021-122954NB-100 funded by MCIN/AEI/10.13039/501100011033 and by "ERDF A way of making Europe." The authors are grateful to the reviewers for their comments and suggestions. Their excellent work help us to improve this paper.

AUTHOR DECLARATIONS

Conflict of Interest

The authors have no conflicts to disclose.

Author Contributions

J. Llibre: Conceptualization (equal); Funding acquisition (equal); Investigation (equal); Methodology (equal); Project administration (equal); Supervision (equal); Writing – original draft (equal); Writing – review & editing (equal). **C. Pantazi:** Conceptualization (equal); Investigation (equal); Methodology (equal); Project administration (equal); Supervision (equal); Writing – original draft (equal); Writing – review & editing (equal).

DATA AVAILABILITY

Data sharing is not applicable to this article as no new data were created or analyzed in this study.

APPENDIX: POINCARÉ COMPACTIFICATION IN $\mathbb{R}^3$.

Poincaré in his classical work (Ref. 15) of 1881 introduced a technique for studying the behavior of the planar vector field in a neighborhood of infinity, see also Refs. 16 and 17. For the extension of this study in higher dimensional vector fields, see Refs. 17 and 18.

Here, we consider the polynomial differential system in $\mathbb{R}^3$,

$$\dot{x} = P_1(x,y,z),\ \dot{y} = P_2(x,y,z),\ \dot{z} = P_3(x,y,z),$$

and its associated vector field

$$X = P_1(x,y,z)\frac{\partial}{\partial x} + P_2(x,y,z)\frac{\partial}{\partial y} + P_3(x,y,z)\frac{\partial}{\partial z}$$

of degree $n = \max\{\deg(P_1), \deg(P_2), \deg(P_3)\}$. We denote by

$$\mathbb{S}^3 = \{y = (y_1,y_2,y_3,y_4) \in \mathbb{R}^4 : ||y|| = 1\},$$

the unit sphere in $\mathbb{R}^4$, and we define the northern and southern hemispheres,

$$\mathbb{S}^{3+} = \{y \in \mathbb{S}^3 : y_4 > 0\}, \quad \mathbb{S}^{3-} = \{y \in \mathbb{S}^3 : y_4 < 0\},$$

respectively. We denote by $T_y\mathbb{S}^3$ the tangent space to $\mathbb{S}^3$ at the point y. Note that the tangent hyperplane $T_{(0,0,0,1)}\mathbb{S}^3 = \{(x_1,x_2,x_3,1) \in \mathbb{R}^4\}$ is identified with $\mathbb{R}^3$. Through the central projections,

$$f^{\pm} : \mathbb{R}^3 = T_{(0,0,0,1)}\mathbb{S}^3 \to \mathbb{S}^{\pm} \quad \text{with} \quad f^{\pm} = \pm\frac{1}{\Delta(x)}(x_1,x_2,x_3,1),$$

the $\mathbb{R}^3$ can be identified with northern and southern hemispheres. Moreover, the equator $\mathbb{S}^2 = \{y \in \mathbb{S}^3 : y_4 = 0\}$ of $\mathbb{S}^3$ can be identified with the infinity of $\mathbb{R}^3$. Here, we denote by $\Delta(x) = \sqrt{1+x_1^2+x_2^2+x_3^2}$. The maps $f^{\pm}$ define two copies of X, one in each hemisphere. We denote by $\bar{X}$ the vector field on $\mathbb{S}^3\setminus\mathbb{S}^2 = \mathbb{S}^+ \cup \mathbb{S}^-$ such that $\bar{X}|_{\mathbb{S}^+} = Df^+ \circ X$ and $\bar{X}|_{\mathbb{S}^-} = Df^- \circ X$.

Now we consider the orthogonal projection of the closed northern hemisphere to $y_4 = 0$, and we obtain the closed ball $\mathbb{B}^3$ of radius one centering at the origin of coordinates. The interior of this ball is diffeomorphic to $\mathbb{R}^3$ and its boundary $\mathbb{S}^2$ is the infinity of $\mathbb{R}^3$.

We need to extend analytically the vector field $\bar{X}$ to the boundary of the ball $\mathbb{B}^3$ in a such a way that the flow on the boundary is invariant. This extention is done with

$$p(X) = y_4^{n-1}\bar{X}(y)$$

and is called the *Poincaré compactification* of X, on the whole ball $\mathbb{B}^3$.

Now we shall give the expressions of $p(X)$ in each local chart of the differential manifold $\mathbb{B}^3$ (for more details on their computations, see Refs. 17 and 18). For this, we consider the eight local charts, (U_i,F_i), (V_i,G_i) for $i = 1,2,3,4$, where $U_i = \{y \in \mathbb{S}^3 : y_i > 0\}$, $V_i = \{y \in \mathbb{S}^3 : y_i < 0\}$, $F_i : U_i \to \mathbb{R}^3$, and $G_i : V_i \to \mathbb{R}^3$ for $i = 1,2,3,4$. The diffeomorphisms F_i, G_i are the inverses of the central projections from the origin to the tangent planes at the points $(\pm1,0,0,0)$, $(0,\pm1,0,0)$, $(0,0,\pm1,0)$, and $(0,0,0,\pm1)$, respectively.

The expression of the analytic vector field $p(X)$ in the chart (U_1,F_1) is

$$p(X) = \frac{z_3^n}{(\Delta(z))^{n-1}}(-z_1P_1 + P_2, -z_2P_1 + P_3, -z_3P_1),$$
$$P_i = P_i\left(\frac{1}{z_3}, \frac{z_1}{z_3}, \frac{z_2}{z_3}\right),\ i = 1,2,3.$$

In the chart (U_2,F_2), we have

$$p(X) = \frac{z_3^n}{(\Delta(z))^{n-1}}(-z_1P_2 + P_1, -z_2P_2 + P_3, -z_3P_2),$$
$$P_i = P_i\left(\frac{z_1}{z_3}, \frac{1}{z_3}, \frac{z_2}{z_3}\right),\ i = 1,2,3,$$

and in the chart (U_3,F_3),

$$p(X) = \frac{z_3^n}{(\Delta(z))^{n-1}}(-z_1P_3 + P_1, -z_2P_3 + P_2, -z_3P_3),$$
$$P_i = P_i\left(\frac{z_1}{z_3}, \frac{z_2}{z_3}, \frac{1}{z_3}\right),\ i = 1,2,3.$$

Now, in the chart (U_4,F_4), we have

$$P(X) = z_3^{n+1}(P_1, P_2, P_3), \quad P_i = P_i(z_1,z_2,z_3),\ i = 1,2,3.$$

In the local charts (V_i,G_i), the expression of the compactified vector field $p(X)$ is the same as in the charts (U_i,F_i) multiplied by the factor $(-1)^{n-1}$. Hence, the infinite equilibrium points appear on pairs

diametrally opposite on $\mathbb{S}^2$ and if n is odd have the same stability while if n is even have the opposite stability.

By a rescaling of the time, we can omit the expression $(\Delta(z))^{n-1}$ in the above expressions of $p(X)$. Note that all the points at infinity in the coordinates of any local chart have $z_3 = 0$. The equilibrium points of $p(X)$ that are on $\mathbb{S}^2$ (the boundary of the ball $\mathbb{B}^3$) are called *infinite equilibrium points*, and the ones that are in the interior of the ball are the *finite equilibrium points*.

REFERENCES

[1]G. L. Oppo and A. Politi, "Toda potential in laser equations," Z. Phys. B Con. Mat. **59**, 111–115 (1985).
[2]F. T. Arecchi, G. L. Lippi, G. P. Puccioni, and J. R. Tredicce, "Deterministic chaos in laser with injected signal," Opt. Commun. **51**, 308–314 (1984).
[3]A. Politi, G. L. Oppo, and R. Badii, "Coexistence of attracting and conservative features in reversible dynamical systems," Stochast. Process. Classical Quantum Syst. **262**, 486–490 (1986).
[4]R. Meucci, J. M. Ginoux, M. Mehrabbeik, S. Jafari, and J. Clinton Sprott, "Generalized multistability and its control in a laser," Chaos **32**, 083111 (2022).
[5]G. L. Oppo, A. Politi, G. L. Lippi, and F. T. Arecchi, "Frequency pushing in lasers with injected signal," Phys. Rev. A **34**, 4000 (1986).
[6]H. G. Solari and G. L. Oppo, "Laser with injected signal: Perturbation of an invariant circle," Opt. Commun. **111**, 173–190 (1994).
[7]M. G. Zimmermann, M. A. Natiello, and H. G. Solari, "Silnikov–saddle–node interaction near a codimension-2 bifurcation: Laser with injected signal," Physica D **109**, 293–314 (1997).
[8]M. G. Zimmermann, M. A. Natiello, and H. G. Solari, "Global bifurcations in a laser with injected signal: Beyond Adler's approximation," Chaos **11**, 500–513 (2001).
[9]A. Politi, G. L. Oppo, and R. Badii, "Coexistence of conservative and dissipative behavior in reversible dynamical systems," Phys. Rev. A **33**, 4055 (1986).
[10]A. I. Amen, "Integrability and dynamics analysis of the chaos laser system," Sci. Iran. (published online 2023).
[11]Y. Li, M. Yuan, and Z. Chen, "Multi-parameter analysis of transition from conservative to dissipative behaviors for a reversible dynamic system," Chaos, Solitons Fractals **159**, 112114 (2022).
[12]M. F. Singer, "Liouvillian first integrals of differential equations," Trans. Am. Math. Soc. **333**, 673–688 (1962).
[13]M. Toda, "Studies of a non–linear lattice," Phys. Rep. **18**, 1–123 (1975).
[14]A. Denjoy, "Sur les courbes définies par les équations différentielles à la surface du tore," J. Math. Pure Appl. **11**, 333–376 (1932).
[15]H. Poincaré, "Memoire sur les courbes definies par une equation diffirentielle," J. Math. **7**, 375–422 (1881).
[16]F. Dumortier, J. Llibre, and J. C. Artés, *Qualitative Theory of Planar Polynomial Systems* (Springer, New York, 2006).
[17]E. A. G. Velasco, "Generic properties of polynomial vector fields at infinity," Trans. Am. Math. Soc. **143**, 201–222 (1969).
[18]A. Cima and J. Llibre, "Bounded polynomial vector fields," Trans. Am. Math. Soc. **318**, 557–579 (1990).